

η_c - and J/Ψ -nucleus bound statesJ.J. Cobos-Martínez^{a,*}, K. Tsushima^b, G. Krein^c, A.W. Thomas^d^a*Cátedra CONACyT, Departamento de Física, Centro de Investigación y de Estudios Avanzados del Instituto Politécnico Nacional, Apartado Postal 14-740, 07000, Ciudad de México, México*^b*Laboratório de Física Teórica e Computacional-LFTC, Universidade Cidade de São Paulo, 01506-000, São Paulo, SP, Brazil*^c*Instituto de Física Teórica, Universidade Estadual Paulista, Rua Dr. Bento Teobaldo Ferraz, 271 - Bloco II, 01140-070, São Paulo, SP, Brazil*^d*CSSM, School of Chemistry and Physics, University of Adelaide, Adelaide SA 5005, Australia***Abstract**

η_c - and J/Ψ -nucleus bound state energies are calculated for various nuclei. Essential input for the calculations, namely the medium-modified D and D^* meson masses, as well as the density distributions in nuclei, are calculated within the quark-meson coupling (QMC) model. The attractive potentials for the η_c and J/Ψ mesons in the nuclear medium originate, respectively, from the in-medium enhanced DD^* and $D\bar{D}$ loops in the η_c and J/Ψ self energies. Our results suggest that the η_c and J/Ψ mesons should form bound states with all the nuclei considered when they are produced at rest inside the nucleus.

1. Introduction

The study of the interactions of charmonium states, such as η_c and J/Ψ , with atomic nuclei offers opportunities to gain new insight into the properties of the strong force and strongly interacting matter [1, 2]. Because charmonia and nucleons do not share light quarks, the Zweig rule suppresses interactions mediated by the exchange of mesons made of light quarks. It is therefore vital to explore other potential sources of attraction which could potentially lead to binding of charmonia to atomic nuclei.

A large body of work looking for alternatives to the meson-exchange paradigm has accumulated over the last three decades [3, 4, 5, 6]. There are works based on the charmonium color polarizability [7, 8], responsible for long-range van der Waals type of forces [9, 10, 12, 11, 13, 14, 15, 16]. Others employ charmed meson loops, with light quarks created from the vacuum [13, 17, 19, 18, 20]. There are studies based on QCD sum rules [21, 22, 23, 24] and phenomenological potentials [25, 26]. More recently, there appeared lattice QCD simulations of the binding of charmonia to nuclear

matter finite nuclei [27], as well as light mesons and baryons [28]. The lattice QCD simulations of Ref. [27] have demonstrated that quarkonium-nucleus bound states exist for $A < 5$. Ref. [27] also infers a charmonium-nuclear matter binding energy $B^{NM} \sim 60$ MeV. However, these simulations have been performed at the flavor $SU(3)$ -symmetric point, with unphysical pion masses, $m_\pi \sim 805$ MeV.

Model studies have suffered from scarce experimental data on the low-energy charmonium-nucleon interaction. However, this situation started to change with the recent measurement, by the JLab GlueX Collaboration [29], of the $\gamma p \rightarrow J/\Psi p$ total cross section near threshold. It will further improve with the completion of other close-to-threshold J/Ψ photoproduction experiments at JLab [30, 31]. Regarding production on nuclei, there is a JLab proposal to measure J/Ψ photoproduction off the deuteron [32]. From the theory side, lattice QCD simulations of the free-space charmonium-nucleon interaction have become available within the last decade [33, 34, 35, 36, 37]. Unfortunately they have either been quenched or used large pion masses, which therefore require extrapolation to the physical mass [16].

Although crucial for constraining models, experimental knowledge of the free-space charmonium-

*Corresponding author

Email addresses: jacobos@fis.cinvestav.mx (J.J. Cobos-Martínez), kazuo.tsushima@gmail.com (K. Tsushima), gkrein@ift.unesp.br (G. Krein), anthony.thomas@adelaide.edu.au (A.W. Thomas)

nucleon interaction is not enough for assessing the likelihood of charmonium binding in nuclei. The overwhelming evidence that the internal structure of hadrons changes in medium [38, 39, 4, 6] must be taken into account when addressing charmonium in nuclei. As shown in previous studies [13, 17, 19, 18, 20], the effect of the nuclear mean fields on subthreshold $D\bar{D}$ states is of particular relevance. Those studies have revealed that modifications induced by the strong nuclear mean fields on the D mesons' light-quark content enhance the self-energy in such a way as to provide an attractive J/Ψ -nucleus effective potential. In the present paper we extend and update our previous study on the J/Ψ -nucleus bound states [17, 19] to the case of η_c charmonium. η_c -nucleus bound states have also been predicted in other approaches [1, 2, 11, 21, 24], albeit with predictions for the binding energies varying over a wide range.

It is worth stressing that compared to the situation for the lighter ϕ meson [40, 41, 42, 43, 44, 45, 46, 47, 48, 49], which couples strongly to above-threshold $K\bar{K}$ states, the charmonium states are expected to have a small width in medium. Moreover, since charmonia are heavier than the ϕ meson, they are expected to move slower than the ϕ meson once produced near threshold inside a nucleus. As a result, one might expect charmonia to have a larger probability to form nuclear bound states than the ϕ meson, while the signal for the formation of such bound states may be experimentally cleaner.

This paper is organized as follows. In Sec. 2 we discuss the computation and present results for the mass shift of the η_c in symmetric nuclear matter. Using the results of Sec. 2, together with the density profiles of the nuclei calculated within the quark meson coupling model, in Sec. 3 we present results for the scalar η_c -nucleus potentials, as well as the corresponding bound state energies. In Sec. 4 we give our updated results for the mass shift of the J/Ψ meson in symmetric nuclear matter, the results for the scalar J/Ψ -nucleus potentials and the corresponding bound state energies. Finally, Sec. 5 is devoted to a summary and conclusions.

2. Calculation of the η_c and J/Ψ scalar potentials in symmetric nuclear matter

For the computation of the η_c and J/Ψ scalar potentials in nuclear matter we use an effective Lagrangian approach at the hadronic level [50]. The

interaction terms for the $\eta_c DD^*$ and $J/\Psi DD$ vertices are given by

$$\mathcal{L}_{\eta_c DD^*} = ig_{\eta_c DD^*} (\partial_\mu \eta_c) [\bar{D}^{*\mu} \cdot D - \bar{D} \cdot D^{*\mu}] \quad (1)$$

$$\mathcal{L}_{\psi DD} = ig_{\psi DD} \psi^\mu [\bar{D} \cdot (\partial_\mu D) - (\partial_\mu \bar{D}) \cdot D], \quad (2)$$

where we have denoted the J/Ψ vector field by ψ , $D^{(*)}$ represents the $D^{(*)}$ -meson field isospin doublet, and $g_{\eta_c DD^*}$ and $g_{\psi DD}$ are coupling constants to be specified below.

The interaction Lagrangians in Eqs. (1)-(2) belong to a set that is an $SU(4)$ extension of light-flavor chiral-symmetric Lagrangians of pseudoscalar and vector mesons. In the light flavor u and d quark sector, they have been motivated by a local gauge symmetry principle, treating vector mesons either as massive gauge bosons or as dynamically generated gauge bosons. Then local gauge symmetry demands the contact interaction $\mathcal{L}_{CI} = g_{\psi D \bar{D}^2} \psi_\mu \psi^\mu D \bar{D}$ term, involving two pseudoscalar mesons and two vector mesons. On the other hand, the effective interaction Lagrangian without the contact term may be considered as being motivated by the hidden gauge approach [51, 52]. This is in contrast to the approach of using the minimal substitution to introduce vector mesons as gauge particles where such four-point vertices do appear. These two methods have been shown to be consistent if both the vector and axial vector mesons are included [53, 54, 55, 56]. Thus, for the vector meson case, we provide results without \mathcal{L}_{CI} .

We use the effective interaction Lagrangians in Eqs. (1)-(2) to compute the η_c and J/Ψ self energies in vacuum and symmetric nuclear matter, following our previous works [17, 18, 19, 20, 45, 46, 47, 48, 49]. In this section we focus on the η_c meson.

Using Eq. (1), and considering only the would be dominant DD^* loop, the η_c self-energy is given by

$$\Sigma_{\eta_c}(k^2) = \frac{4g_{\eta_c DD^*}^2}{\pi^2} \int_0^\infty dk k^2 I(k^2) \quad (3)$$

for an η_c at rest, where

$$I(k^2) = \frac{m_{\eta_c}^2 (-1 + k^{02}/m_{D^*}^2)}{(k^0 + \omega_{D^*})(k^0 - \omega_{D^*})(k^0 - m_{\eta_c} - \omega_D)} \Big|_{k^0=m_{\eta_c}-\omega_{D^*}} + \frac{m_{\eta_c}^2 (-1 + k^{02}/m_{D^*}^2)}{(k^0 - \omega_{D^*})(k^0 - m_{\eta_c} + \omega_D)(k^0 - m_{\eta_c} - \omega_D)} \Big|_{k^0=-\omega_{D^*}}, \quad (4)$$

and $\omega_{D^{(*)}} = (k^2 + m_{D^{(*)}}^2)^{1/2}$, with $k = |\vec{k}|$. The integral in Eq. (3) is divergent and thus needs regularization. For this purpose we employ a phenomenological vertex form factor

$$u_{D^{(*)}}(k^2) = \left(\frac{\Lambda_{D^{(*)}}^2 + m_{\eta_c}^2}{\Lambda_{D^{(*)}}^2 + 4\omega_{D^{(*)}}^2(k^2)} \right)^2, \quad (5)$$

with cutoff parameter $\Lambda_{D^{(*)}}$, as in Refs. [17, 18, 19, 20, 45, 46, 47, 48, 49]. Thus, to regularize Eq. (3) we will introduce the factor $u_D(k^2)u_{D^*}(k^2)$ into the integrand. The main uncertainty here is the value of the cutoff mass Λ_D (for simplicity we use $\Lambda_{D^*} = \Lambda_D$). In a simple-minded picture of the vertices, the cutoff masses are related to the extension of the overlap region of the mesons participating in the vertex and therefore should depend on the spatial distributions of the wave functions of these mesons. One can estimate an approximate value of Λ_D by using a quark model calculation of the form factors [17]. Using a 3P_0 model for quark-pair creation and Gaussian wave functions for the mesons, an expression for the vertex form factor can be written down [17]. By requiring that this quark model form factor and the more phenomenological form factor of Eq. (5) have the same root mean square radii, an estimate for Λ_D was obtained in Ref. [17]: $\Lambda \approx 2500$ MeV. This is indeed a rough estimate but it serves as a reasonable guide to the order of magnitude of Λ_D . In view of this, the sensitivity of the results to the cutoff value is analyzed below, by allowing the cutoff mass Λ_D to vary in the range $1500 \leq \Lambda_D \leq 3000$ MeV.

Because $SU(4)$ flavor symmetry is strongly broken in Nature, we use experimental values for the meson masses [57] and empirically known values for the coupling constants, as explained below. For the D meson mass, we take the averaged masses of the neutral and charged states, and similarly for the D^* . Thus $m_D = 1867.2$ MeV and $m_{D^*} = 2008.6$ MeV. For the coupling constants we use $g_{\psi DD} = 7.64$ and $g_{\eta_c DD^*} = 0.60g_{\psi DD}$, where the former value was obtained in Ref. [58] using the vector meson dominance model and isospin symmetry. The latter relation is motivated by a recent calculation in Ref. [59], as the residue at the poles of suitable form factors using a dispersion formulation of the relativistic constituent quark model. We mention that recent investigations of $SU(4)$ flavor symmetry breaking in hadron couplings of charmed hadrons to light mesons are not conclusive; while two stud-

ies based on Schwinger-Dyson equations of QCD find large deviations from $SU(4)$ symmetry [60, 61], studies using QCD sum rules [62, 63], a constituent quark model [64] and a holographic QCD model [65] find moderate deviations.

We are interested in the difference between the in-medium, $m_{\eta_c}^*$, and vacuum, m_{η_c} , masses of the η_c ,

$$\Delta m_{\eta_c} = m_{\eta_c}^* - m_{\eta_c}, \quad (6)$$

with the masses obtained self-consistently from

$$m_{\eta_c}^2 = (m_{\eta_c}^0)^2 + \Sigma_{\eta_c}(k^2 = m_{\eta_c}^2), \quad (7)$$

where $m_{\eta_c}^0$ is the bare η_c mass and $\Sigma_{\eta_c}(k^2)$ is given by Eq. (3). The Λ_D -dependent η_c -meson bare mass, $m_{\eta_c}^0$, is fixed by fitting the physical η_c -meson mass, $m_{\eta_c} = 2983.9$ MeV.

The in-medium η_c mass is obtained similarly, with the self-energy calculated with the medium-modified D and D^* masses. The nuclear density dependence of the η_c -meson mass is driven by the intermediate-state D and D^* meson interactions with the nuclear medium through their medium-modified masses. The in-medium masses m_D^* and $m_{D^*}^*$ are calculated within the quark-meson coupling (QMC) model [17, 18], in which effective scalar and vector meson mean fields couple to the light u and d quarks in the charmed mesons [17, 18]. The QMC model has proven to be very successful in studying the properties of hadrons in nuclear matter and finite nuclei [69, 70, 66, 67, 68]. This model considers infinitely large, uniformly symmetric, spin-isospin-saturated nuclear matter in its rest frame, where all the scalar and vector mean field potentials, which are responsible for the nuclear many-body interactions, become constant in the Hartree approximation [69, 70, 66].

In Fig. 1 we present the resulting medium-modified masses for the D and D^* mesons, calculated within the QMC model, as a function of ρ_B/ρ_0 , where ρ_B is the baryon density of nuclear matter and $\rho_0 = 0.15 \text{ fm}^{-3}$ is the saturation density of symmetric nuclear matter. The net reductions in the masses of the D and D^* mesons are nearly the same as a function of density, with each decreasing by around 60 MeV at ρ_0 .

The behaviour of the D meson mass in medium (finite density and/or temperature) has been studied in a variety of approaches. Some of these [71, 72, 73] find a decreasing D meson mass at finite baryon density, while others [74, 75, 76, 77, 78], interest-

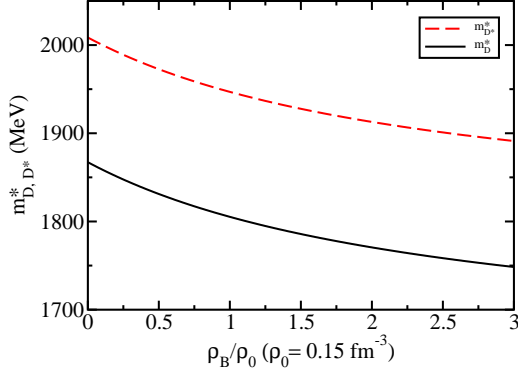


Figure 1: In-medium D and D^* meson masses calculated within the QMC model.

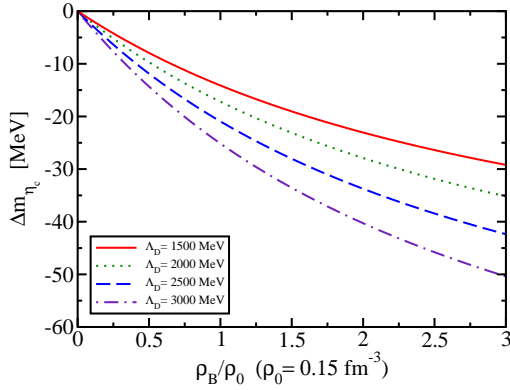


Figure 2: η_c mass shift as a function of the nuclear matter density for various values of the cutoff parameter.

ingly, find the opposite behaviour. However, it is important to note that none of the studies in nuclear matter are constrained by the saturation properties of nuclear matter, although it is constrained in the case of the present work. Furthermore, some of these works employ a non relativistic approach and relativistic effects might be important.

In Fig. 2, we present the η_c -meson mass shift, Δm_{η_c} , as a function of the nuclear matter density, ρ_B , normalized to ρ_0 , for four values of the cutoff parameter Λ_D . As can be seen from the figure, the effect of the in-medium D and D^* mass change is to shift the η_c mass downwards. This is because the reduction in the D and D^* masses enhances the DD^* -loop contribution in nuclear matter relative to that in vacuum. This effect increases the larger

the cutoff mass Λ_D . Some values for the η_c mass shift for various values of the nuclear matter density and cutoff parameter are given in Table 1. The

ρ_B/ρ_0	$\Lambda_D = 1500$	$\Lambda_D = 2000$	$\Lambda_D = 2500$	$\Lambda_D = 3000$
0.5	-7.9	-9.7	-11.9	-14.3
1.0	-14.1	-17.2	-20.9	-25.1
1.5	-19.0	-23.1	-28.0	-33.6
2.0	-23.1	-27.9	-33.7	-40.3
2.5	-26.4	-31.9	-38.4	-45.8
3.0	-29.2	-35.2	-42.4	-50.4

Table 1: η_c mass shift at various values of the nuclear matter density ρ_B/ρ_0 for different values Λ_D . All dimensionful quantities are given in MeV.

results described above support a small downward mass shift for the η_c in nuclear matter and open the possibility to study the binding of η_c mesons to nuclei, to which we turn our attention in the next section.

3. η_c -nucleus bound states

We now discuss the situation where the η_c -meson is produced inside a nucleus A with baryon density distribution $\rho_B^A(r)$. The nuclei we consider here are ${}^4\text{He}$, ${}^{12}\text{C}$, ${}^{16}\text{O}$, ${}^{40}\text{Ca}$, ${}^{48}\text{Ca}$, ${}^{90}\text{Zr}$, ${}^{197}\text{Au}$, and ${}^{208}\text{Pb}$. Their nuclear density distribution are also calculated within the QMC model, except for ${}^4\text{He}$, whose parametrization was obtained in Ref. [79]. Using a local density approximation, the η_c -meson potential within nucleus A is given by

$$V_{\eta_c A}(r) = \Delta m_{\eta_c}(\rho_B^A(r)), \quad (8)$$

where r is the distance from the center of the nucleus.

In Fig. 3 we present the η_c -meson potentials for a selection of the nuclei mentioned above and various values of the cutoff parameter Λ_D . From the figure one can see that the η_c potential in nuclei is attractive in all cases but its depth depends on the value of the cutoff parameter, being deeper the larger Λ_D is. For example, it varies, from -18 MeV to -32 MeV for ${}^4\text{He}$ and from -15 MeV to -26 MeV for ${}^{208}\text{Pb}$, when the cutoff varies from 1500 MeV to 3000 MeV. This dependence is, indeed, an uncertainty in the results obtained in our approach.

Using the η_c -meson potentials obtained in this manner, we next calculate the η_c -meson-nucleus bound state energies for the nuclei listed above by solving the Klein-Gordon equation

$$(-\nabla^2 + \mu^2 + 2\mu V(\vec{r}))\phi_{\eta_c}(\vec{r}) = \mathcal{E}^2\phi_{\eta_c}(\vec{r}), \quad (9)$$

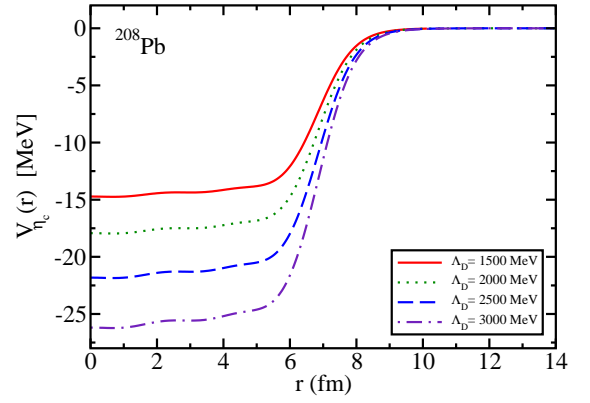
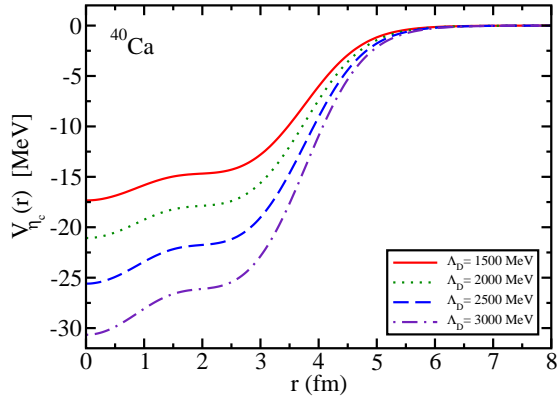
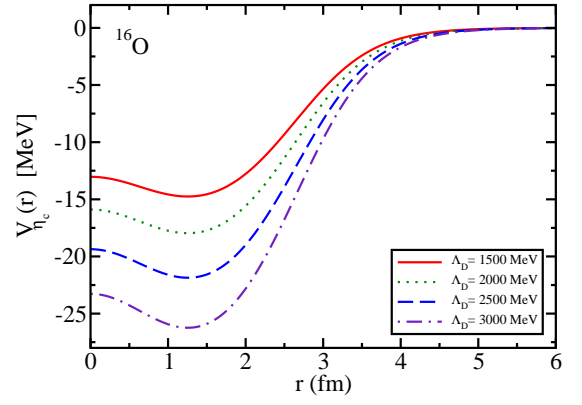
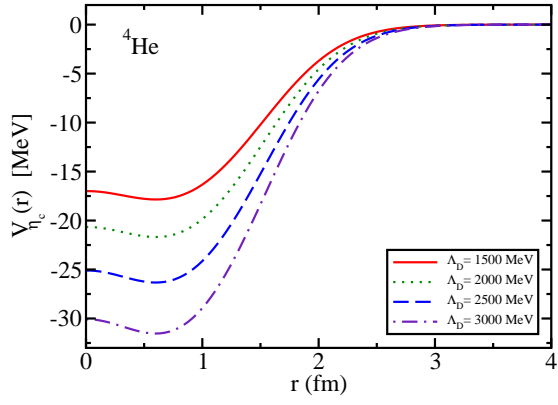


Figure 3: η_c -nucleus potentials for various nuclei and values of the cutoff parameter Λ_D .

		Bound state energies			
$n\ell$		$\Lambda_D = 1500$	$\Lambda_D = 2000$	$\Lambda_D = 2500$	$\Lambda_D = 3000$
^4He	1s	-1.49	-3.11	-5.49	-8.55
$^{12}_{\eta_c}\text{C}$	1s	-5.91	-8.27	-11.28	-14.79
	1p	-0.28	-1.63	-3.69	-6.33
$^{16}_{\eta_c}\text{O}$	1s	-7.35	-9.92	-13.15	-16.87
	1p	-1.94	-3.87	-6.48	-9.63
$^{40}_{\eta_c}\text{Ca}$	1s	-11.26	-14.42	-18.31	-22.73
	1p	-7.19	-10.02	-13.59	-17.70
	1d	-2.82	-5.22	-8.36	-12.09
	2s	-2.36	-4.51	-7.44	-10.98
$^{48}_{\eta_c}\text{Ca}$	1s	-11.37	-14.46	-18.26	-22.58
	1p	-7.83	-10.68	-14.23	-18.32
	1d	-3.88	-6.40	-9.63	-13.41
	2s	-3.15	-5.47	-8.54	-12.17
$^{90}_{\eta_c}\text{Zr}$	1s	-12.26	-15.35	-19.14	-23.43
	1p	-9.88	-12.86	-16.53	-20.70
	1d	-7.05	-9.87	-13.38	-17.40
	2s	-6.14	-8.87	-12.29	-16.24
	1f	-3.90	-6.50	-9.81	-13.65
$^{197}_{\eta_c}\text{Au}$	1s	-12.57	-15.59	-19.26	-23.41
	1p	-11.17	-14.14	-17.77	-21.87
	1d	-9.42	-12.31	-15.87	-19.90
	2s	-8.69	-11.53	-15.04	-19.02
	1f	-7.39	-10.19	-13.70	-17.61
$^{208}_{\eta_c}\text{Pb}$	1s	-12.99	-16.09	-19.82	-24.12
	1p	-11.60	-14.64	-18.37	-22.59
	1d	-9.86	-12.83	-16.49	-20.63
	2s	-9.16	-12.09	-15.70	-19.80
	1f	-7.85	-10.74	-14.30	-18.37

Table 2: η_c -nucleus bound state energies for different values of the cutoff parameter Λ_D . All dimensionful quantities are in MeV.

where $\mu = m_{\eta_c} m_A / (m_{\eta_c} + m_A)$ is the reduced mass of the η_c -meson-nucleus system with m_{η_c} (m_A) the mass of the η_c -meson (nucleus A) in vacuum, and $V(\vec{r})$ is the η_c -meson-nucleus potential given in Eq. (8).

The bound state energies (E) of the η_c -nucleus system, given by $E = \mathcal{E} - \mu$, where \mathcal{E} is the energy eigenvalue in Eq. (9), are calculated for four values of the cutoff parameter Λ_D and are listed in Table 2. These results show that the η_c -meson is expected to form bound states with all the nuclei studied and this prediction is independent of the value of the cutoff parameter Λ_D . However, the particular values for the bound state energies are clearly dependent on Λ_D , namely, each of them increases in absolute value as Λ_D increases. This was expected from the behavior of the η_c potentials, since these are deeper for larger values of the cutoff parameter. Note also that the η_c binds more strongly to heavier nuclei. We have also solved the Schrödinger equation with the potential Eq. (8) to obtain the single-particle energies [6] and compared these with those given in Table 2. The results found

in both cases are essentially the same.

4. J/Ψ -nucleus bound states

Using an effective Lagrangian approach (see Eq. (2)), together with the QMC model to compute the nuclear density dependence of the D and D^* meson masses (see Fig. 1), the J/Ψ mass shift in nuclear matter and J/Ψ -nucleus bound states were studied in Refs. [17, 18, 19, 20]. In these studies, the J/Ψ self-energy involved the D , \bar{D} , D^* , and \bar{D}^* mesons as intermediate states. However, it turned out that the J/Ψ self-energy gave a larger contribution from the loops involving the D^* and \bar{D}^* mesons.

This at first sight is unexpected, since the mass of the D^* (\bar{D}^*) is heavier than that of the D (\bar{D}) meson by about 140 MeV in vacuum, and the decrease of their masses in nuclear matter is nearly the same for these mesons [17, 18, 19, 20], see Fig. 1. This is probably associated with the known, bad high-energy behavior of the vector meson propagators which appear in the self-energy calculation. In the case of the most famous spontaneously broken gauge theory, the Standard Model, this bad high-energy behavior is tamed by using the 't Hooft-Feynman gauge ($\xi = 1$ in R_ξ gauge), which makes the behavior of the gauge boson (W^\pm, Z^0) propagators similar to those of (pseudo)scalar mesons [80, 81, 82, 83]. This removes unphysical Goldstone-boson degrees of freedom. In the present case, we cannot justify the use of such vector meson propagators. It is also important to note that in those studies, the coupling constants for the $J/\Psi DD^*$ and $J/\Psi D^* D^*$ vertices were assumed to be the same as those for the $J/\Psi D \bar{D}$ vertex. Furthermore, no cutoff readjustments were made for the heavier intermediate states involving the D^* mesons; that is, the same cutoff (Λ_D) was used in all vertex form factors. This latter issue, in particular, should play an important role, as heavier intermediate states induce fluctuations from shorter distances and a accompanying readjustment of the corresponding cutoff might be required to compensate for such fluctuations. These issues call for further investigations in the future.

In the meantime, the following updated results for the J/Ψ meson in nuclear matter and nuclei are obtained by considering only the lightest intermediate state in the J/Ψ self-energy, namely the $D \bar{D}$ loop. The approach used for this is the same as we used for the η_c and in previous works; namely, we

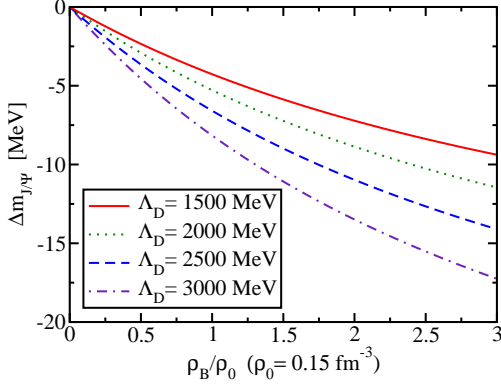


Figure 4: J/Ψ mass shift as a function of nuclear matter density for various values of the cutoff parameter.

use the effective Lagrangian of Eq. (2) to compute the J/Ψ self energy in vacuum and in-medium, for a J/Ψ at rest, and the QMC model to provide the nuclear density dependence of the D and \bar{D} meson masses (see Fig. 1), and the density distributions of the nuclei considered. Thus, our estimates may be regarded as including the minimum contributions concerning the intermediate state meson loops.

ρ_B/ρ_0	$\Lambda_D = 1500$	$\Lambda_D = 2000$	$\Lambda_D = 2500$	$\Lambda_D = 3000$
0.5	-2.3	-2.9	-3.7	-4.5
1.0	-4.3	-5.3	-6.6	-8.2
1.5	-5.9	-7.2	-9.0	-11.1
2.0	-7.2	-8.9	-11.0	-13.5
2.5	-8.4	-10.3	-12.7	-15.5
3.0	-9.4	-11.5	-14.1	-17.3

Table 3: J/Ψ mass shift at various values of the nuclear matter density ρ_B/ρ_0 for different values Λ_D . All dimensional quantities are given in MeV.

In Fig. 4, we present the J/Ψ mass shift, $\Delta m_{J/\Psi}$, as a function of the nuclear matter density, ρ_B , for four values of the cutoff parameter Λ_D . See also Table 3 for some particular values. These results show a negative mass shift (attractive potential) for the J/Ψ in symmetric nuclear matter in all cases. This is in line with the results based on the polarizability of charmonium [6] and also with those on the QCD sum rules of Refs. [21, 22, 23, 24] that find a negative mass shift in the range $3 \text{ MeV} \leq |\Delta m_{J/\Psi}| \leq 10 \text{ MeV}$. But they are somewhat smaller than those of a recent Lattice calculation in Ref. [27].

A negative mass shift means that the nuclear medium provides attraction to the J/Ψ , allowing for the possibility of bound state formation between

the J/Ψ and a nucleus. In Fig. 5 we present the J/Ψ -meson potentials calculated for the same nuclei as in the η_c case and same values of the cutoff parameter Λ_D . From the figure one can see that the J/Ψ potential in nuclei is attractive in all cases but its depth is sensitive to the value of the cutoff parameter, being deeper for larger values of Λ_D . As we will show below, the J/Ψ potentials are attractive enough to allow the formation of the J/Ψ -meson bound states with nuclei. For example, it varies, from -5.5 MeV to -10.4 MeV for ^4He and from -4.5 MeV to -8.5 MeV for ^{208}Pb , when the cutoff varies from 1500 MeV to 3000 MeV. The sensitivity of our results on the cutoff is studied below.

As mentioned above, we provide results for the J/Ψ -nucleus bound states including only the $D\bar{D}$ loop in the J/Ψ self-energy. For a spin-1 massive particle subject to a scalar potential the Proca equation must be solved. However, for a J/Ψ meson produced at rest (recoilless kinematics in experiments), it should be a very good approximation to neglect the possible energy difference between the longitudinal and transverse components of the J/Ψ wave function (ϕ_ψ^μ) [18, 46, 84]. After imposing the Lorentz condition, $\partial_\mu \phi_\psi^\mu$, to solve the Proca equation becomes equivalent to solving the Klein-Gordon equation Eq. (9).

		Bound state energies (E)			
		$\Lambda_D = 1500$	$\Lambda_D = 2000$	$\Lambda_D = 2500$	$\Lambda_D = 3000$
$^4_{J/\Psi}\text{He}$	1s	n	n	-0.01	-0.02
$^{12}_{J/\Psi}\text{C}$	1s	-0.18	-0.53	-1.12	-1.99
$^{16}_{J/\Psi}\text{O}$	1s	-0.52	-1.03	-1.81	-2.87
$^{40}_{J/\Psi}\text{Ca}$	1s	-1.92	-2.78	-3.96	-5.45
	1p	n	-0.38	-1.18	-2.32
$^{48}_{J/\Psi}\text{Ca}$	1s	-2.09	-2.97	-4.15	-5.62
	1p	-0.16	-0.73	-1.62	-2.83
$^{90}_{J/\Psi}\text{Zr}$	1s	-2.70	-3.65	-4.89	-6.41
	1p	-1.13	-1.93	-3.03	-4.43
	1d	n	-0.08	-0.94	-2.13
	2s	n	-0.02	-0.56	-1.56
$^{197}_{J/\Psi}\text{Au}$	1s	-3.14	-4.09	-5.33	-6.84
	1p	-2.10	-2.98	-4.16	-5.61
	1d	-0.86	-1.66	-2.74	-4.11
	2s	-0.53	-1.23	-2.24	-3.54
	1f	n	-0.20	-1.15	-2.40
$^{208}_{J/\Psi}\text{Pb}$	1s	-3.28	-4.26	-5.53	-7.08
	1p	-2.24	-3.16	-4.38	-5.87
	1d	-1.02	-1.84	-2.97	-4.38
	2s	-0.67	-1.41	-2.47	-3.83
	1f	n	-0.39	-1.39	-2.69

Table 4: J/Ψ -meson-nucleus bound state energies, calculated from the Klein-Gordon equation. When $|E| < 10^{-2}$ MeV we consider there is no bound state, which we denote with “n”. All dimensional quantities are in MeV.

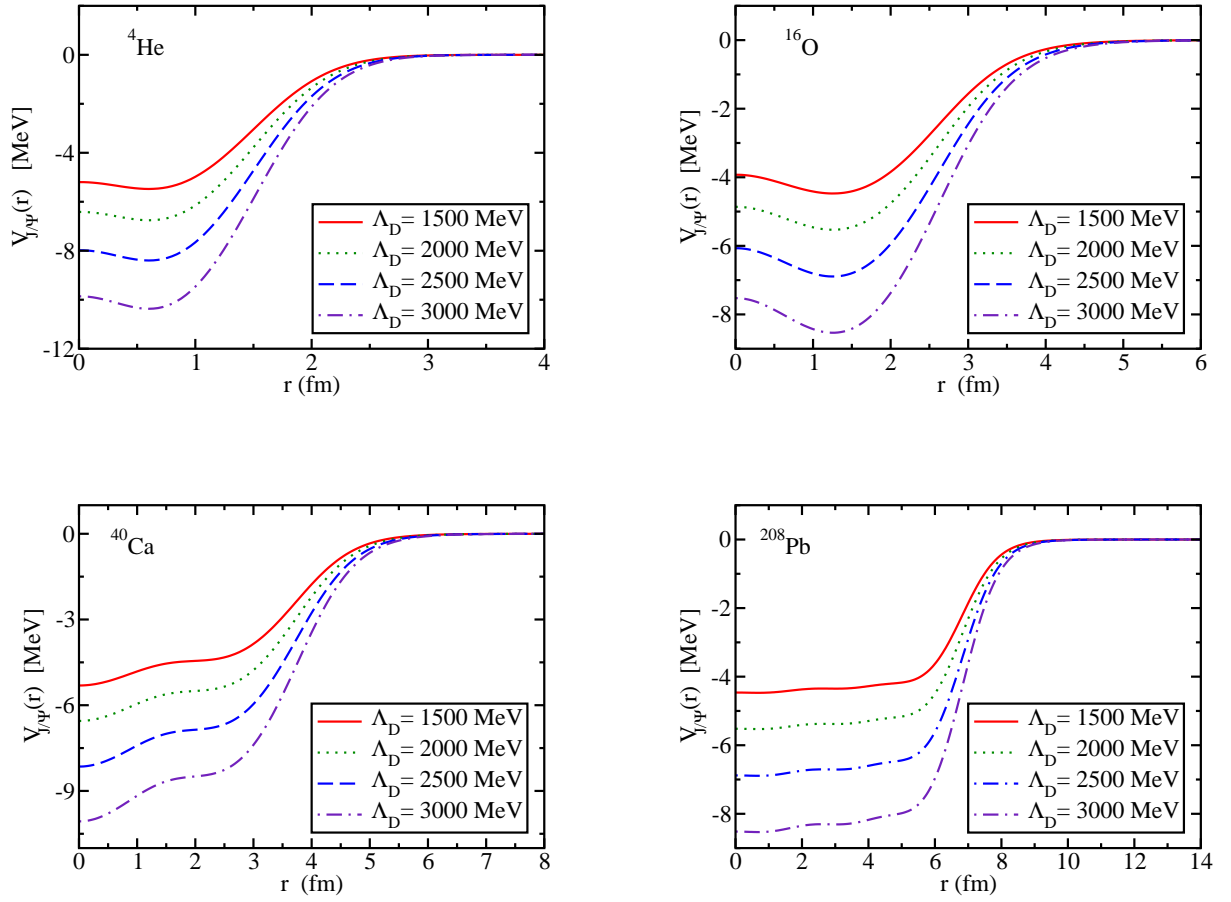


Figure 5: J/Ψ -nucleus potentials for various nuclei and values of the cutoff parameter Λ_D .

The bound state energies for the J/Ψ meson for various nuclei are listed in Table 4. These results show that the J/Ψ is expected to form J/Ψ -nucleus bound states for nearly all the nuclei considered, but only in some cases for ${}^4\text{He}$. This is insensitive to the values of the cutoff used in the form factor. Thus, it will be possible to search for the bound states in a ${}^{208}\text{Pb}$ nucleus at JLab now that the 12 GeV upgrade has been completed. In addition, one can expect a rich spectrum of states for medium and heavy mass nuclei. Of course, the main issue is to produce the J/Ψ meson with nearly stopped kinematics, or nearly zero momentum relative to the nucleus. Since the present results imply that many nuclei should form J/Ψ -nuclear bound states, it may be possible to find such kinematics by careful selection of the beam and target nuclei.

5. Summary and discussion

We have calculated the spectra of η_c - and J/Ψ -nucleus bound states for various finite nuclei. The meson-nucleus potentials were calculated using a local density approximation, with the inclusion of the DD^* ($D\bar{D}$) meson loop in the η_c (J/Ψ) self-energy. The nuclear density distributions, as well as the in-medium D and D^* meson masses were consistently calculated by employing the quark-meson coupling model. Using the meson potentials in nuclei, we have solved the Klein-Gordon equation and obtained meson-nucleus bound state energies. The sensitivity of our results to the cutoff parameter Λ_D used in the vertex form factors appearing in the η_c (J/Ψ) self-energy has also been explored.

Our results show that one should expect the η_c and J/Ψ to form bound states for all the nuclei studied, provided that the mesons are produced in (nearly) recoilless kinematics, even though the precise values of the bound state energies are dependent on the cutoff mass values used in the form factors. The discovery of such bound states would represent an important step forward in our understanding of the nature of strongly interacting systems.

Acknowledgements

This work was partially supported by Conselho Nacional de Desenvolvimento Científico e

Tecnológico (CNPq), process Nos. 313063/2018-4 (KT), 426150/2018-0 (KT) and 309262/2019-4 (GK), and Fundação de Amparo à Pesquisa do Estado de São Paulo (FAPESP) process Nos. 2019/00763-0 (KT), 64898/2014-5 (KT) and 2013/01907-0 (GK). The work is also part of the project Instituto Nacional de Ciência e Tecnologia – Nuclear Physics and Applications (INCT-FNA), process. No. 464898/2014-5 (KT, GK). It was also supported by the Australian Research Council through DP180100497 (AWT).

References

- [1] S. J. Brodsky, I. Schmidt and G. de Teramond, Phys. Rev. Lett. **64** (1990), 1011
- [2] D. Wasson, Phys. Rev. Lett. **67** (1991), 2237
- [3] A. Hosaka, T. Hyodo, K. Sudoh, Y. Yamaguchi and S. Yasui, Prog. Part. Nucl. Phys. **96** (2017), 88-153
- [4] G. Krein, AIP Conf. Proc. **1701**, no.1, 020012 (2016)
- [5] V. Metag, M. Nanova and E. Y. Paryev, Prog. Part. Nucl. Phys. **97** (2017), 199-260
- [6] G. Krein, A. W. Thomas and K. Tsushima, Prog. Part. Nucl. Phys. **100**, 161 (2018)
- [7] M. E. Peskin, Nucl. Phys. B **156** (1979), 365-390
- [8] D. Kharzeev, Proc. Int. Sch. Phys. Fermi **130** (1996), 105
- [9] A. Kaidalov and P. Volkovitsky, Phys. Rev. Lett. **69** (1992), 3155-3156
- [10] M. E. Luke, A. V. Manohar and M. J. Savage, Phys. Lett. B **288** (1992), 355-359
- [11] G. F. de Teramond, R. Espinoza and M. Ortega-Rodriguez, Phys. Rev. D **58** (1998), 034012
- [12] S. J. Brodsky and G. A. Miller, Phys. Lett. B **412** (1997), 125-130
- [13] S. H. Lee and C. Ko, Phys. Rev. C **67** (2003), 038202
- [14] A. Sibirtsev and M. Voloshin, Phys. Rev. D **71** (2005), 076005.
- [15] M. Voloshin, Prog. Part. Nucl. Phys. **61** (2008), 455-511
- [16] J. Tarrús Castellà and G. Krein, Phys. Rev. D **98** (2018) no.1, 014029
- [17] G. Krein, A. W. Thomas and K. Tsushima, Phys. Lett. B **697** (2011), 136-141
- [18] K. Tsushima, D. Lu, G. Krein and A. W. Thomas, Phys. Rev. C **83** (2011), 065208
- [19] K. Tsushima, D. Lu, G. Krein and A. W. Thomas, AIP Conf. Proc. **1354** (2011) no.1, 39-44
- [20] G. Krein, J. Phys. Conf. Ser. **422**, 012012 (2013).
- [21] F. Klingl, S. s. Kim, S. H. Lee, P. Morath and W. Weise, Phys. Rev. Lett. **82** (1999), 3396 Phys. Rev. Lett. **83** (1999), 4224 (erratum);
- [22] A. Hayashigaki, Prog. Theor. Phys. **101** (1999), 923-935
- [23] S. s. Kim and S. H. Lee, Nucl. Phys. A **679** (2001), 517-548
- [24] A. Kumar and A. Mishra, Phys. Rev. C **82** (2010), 045207
- [25] V. Belyaev, N. Shevchenko, A. Fix and W. Sandhas, Nucl. Phys. A **780** (2006), 100-111
- [26] A. Yokota, E. Hiyama and M. Oka, PTEP **2013** (2013) no.11, 113D01

- [27] S. Beane, E. Chang, S. Cohen, W. Detmold, H. W. Lin, K. Orginos, A. Parreo and M. Savage, Phys. Rev. D **91** (2015) no.11, 114503
- [28] M. Alberti, G. S. Bali, S. Collins, F. Knechtli, G. Moir and W. Sldner, Phys. Rev. D **95** (2017) no.7, 074501
- [29] A. Ali *et al.* [GlueX], Phys. Rev. Lett. **123** (2019) no.7, 072001
- [30] Near Threshold J/ψ Photoproduction and Study of LHCb Pentaquarks with CLAS12, Spokespersons: S. Stepanyan, M. Battaglieri, A. Celentano, R. De Vita, and V. Kubarovsky, JLab E12-12-001A, Newport News, VA, USA, 2012.
- [31] A Search for the LHCb Charmed Pentaquark using Photo-Production of J/ψ at Threshold in Hall C at Jefferson Lab, Z. E. Meziani *et al.*
- [32] Study of J/Ψ Photoproduction off Deuteron, Spokespersons: Y. Ilieva, B. McKinnon, P. Nadel-Turonski, V. Kubarovsky, S. Stepanyan, and Z. W. Zhao, JLab E12-11-003B, Newport News, VA, USA, 2011.
- [33] K. Yokokawa, S. Sasaki, T. Hatsuda and A. Hayashigaki, Phys. Rev. D **74** (2006), 034504
- [34] L. Liu, H. W. Lin and K. Orginos, PoS **LATTICE2008** (2008), 112
- [35] T. Kawanai and S. Sasaki, Phys. Rev. D **82** (2010), 091501
- [36] T. Kawanai and S. Sasaki, PoS **LATTICE2010** (2010), 156
- [37] U. Skerbis and S. Prelovsek, Phys. Rev. D **99** (2019) no.9, 094505.
- [38] R. S. Hayano and T. Hatsuda, Rev. Mod. Phys. **82**, 2949 (2010)
- [39] S. Leupold, V. Metag and U. Mosel, Int. J. Mod. Phys. E **19**, 147 (2010)
- [40] C. M. Ko, P. Levai, X. J. Qiu and C. T. Li, Phys. Rev. C **45** (1992), 1400-1402
- [41] F. Klingl, T. Waas and W. Weise, Phys. Lett. B **431** (1998), 254-262
- [42] E. Oset and A. Ramos, Nucl. Phys. A **679** (2001), 616-628
- [43] D. Cabrera and M. J. Vicente Vacas, Phys. Rev. C **67** (2003), 045203
- [44] P. Gubler and W. Weise, Phys. Lett. B **751** (2015), 396-401
- [45] J. J. Cobos-Martínez, K. Tsushima, G. Krein and A. W. Thomas, Phys. Lett. B **771** (2017), 113-118
- [46] J. J. Cobos-Martínez, K. Tsushima, G. Krein and A. W. Thomas, Phys. Rev. C **96** (2017) no.3, 035201
- [47] J. J. Cobos-Martínez, K. Tsushima, G. Krein and A. W. Thomas, J. Phys. Conf. Ser. **912** (2017) no.1, 012009
- [48] J. J. Cobos-Martínez, K. Tsushima, G. Krein and A. W. Thomas, PoS **Hadron2017** (2018), 209
- [49] J. J. Cobos-Martínez, K. Tsushima, G. Krein and A. W. Thomas, JPS Conf. Proc. **26** (2019), 024033
- [50] F. Klingl, N. Kaiser and W. Weise, Z. Phys. A **356**, 193 (1996)
- [51] Z. w. Lin, C. M. Ko and B. Zhang, Phys. Rev. C **61**, 024904 (2000).
- [52] S. H. Lee, C. Song and H. Yabu, Phys. Lett. B **341**, 407 (1995)
- [53] K. Yamawaki, Phys. Rev. D **35**, 412 (1987).
- [54] U. G. Meissner and I. Zahed, Z. Phys. A **327**, 5 (1987).
- [55] U. G. Meissner, Phys. Rept. **161**, 213 (1988).
- [56] S. Saito and K. Yamawaki, NAGOYA, JAPAN: UNIV., PHYS. DEPT. (1987) 225p
- [57] M. Tanabashi *et al.* [Particle Data Group], Phys. Rev. D **98**, no. 3, 030001 (2018).
- [58] Z. w. Lin and C. M. Ko, Phys. Rev. C **62**, 034903 (2000)
- [59] W. Lucha, D. Melikhov, H. Sazdjian and S. Simula, Phys. Rev. D **93**, no. 1, 016004 (2016); Addendum: [Phys. Rev. D **93**, no. 1, 019902 (2016)]
- [60] B. El-Bennich, G. Krein, L. Chang, C. D. Roberts and D. J. Wilson, Phys. Rev. D **85**, 031502 (2012)
- [61] B. El-Bennich, M. A. Paracha, C. D. Roberts and E. Rojas, Phys. Rev. D **95**, no. 3, 034037 (2017)
- [62] F. S. Navarra and M. Nielsen, Phys. Lett. B **443**, 285 (1998)
- [63] A. Khodjamirian, C. Klein, T. Mannel and Y.-M. Wang, JHEP **1109**, 106 (2011)
- [64] C. E. Fontoura, J. Haidenbauer and G. Krein, Eur. Phys. J. A **53**, no. 5, 92 (2017)
- [65] A. Ballon-Bayona, G. Krein and C. Miller, Phys. Rev. D **96**, no. 1, 014017 (2017)
- [66] K. Saito, K. Tsushima and A. W. Thomas, Prog. Part. Nucl. Phys. **58**, 1 (2007)
- [67] P. A. M. Guichon, H. H. Matevosyan, N. Sandulescu and A. W. Thomas, Nucl. Phys. A **772** (2006), 1-19
- [68] J. R. Stone, P. A. M. Guichon, P. G. Reinhard and A. W. Thomas, Phys. Rev. Lett. **116** (2016) no.9, 092501
- [69] K. Tsushima, K. Saito, A. W. Thomas and S. V. Wright, Phys. Lett. B **429**, 239 (1998) Erratum: [Phys. Lett. B **436**, 453 (1998)]
- [70] P. A. M. Guichon, Nucl. Phys. A **497**, 265C (1989).
- [71] A. Hayashigaki, Phys. Lett. B **487** (2000), 96-103
- [72] K. Azizi, N. Er and H. Sundu, Eur. Phys. J. C **74** (2014), 3021
- [73] Z. G. Wang, Phys. Rev. C **92** (2015) no.6, 065205
- [74] K. Suzuki, P. Gubler and M. Oka, Phys. Rev. C **93** (2016) no.4, 045209
- [75] A. Park, P. Gubler, M. Harada, S. H. Lee, C. Nonaka and W. Park, Phys. Rev. D **93** (2016) no.5, 054035
- [76] P. Gubler, T. Song and S. H. Lee, Phys. Rev. D **101** (2020) no.11, 114029
- [77] T. Hilger, R. Thomas and B. Kampfer, Phys. Rev. C **79** (2009), 025202
- [78] T. F. Caramés, C. E. Fontoura, G. Krein, K. Tsushima, J. Vijande and A. Valcarce, Phys. Rev. D **94** (2016) no.3, 034009
- [79] K. Saito, K. Tsushima and A. W. Thomas, Phys. Rev. C **56**, 566 (1997)
- [80] G. 't Hooft, Nucl. Phys. B **35**, 167 (1971).
- [81] G. 't Hooft, Nucl. Phys. B **33**, 173 (1971).
- [82] B. W. Lee, Phys. Rev. D **5**, 823 (1972).
- [83] K. Fujikawa, B. W. Lee and A. I. Sanda, Phys. Rev. D **6**, 2923 (1972).
- [84] K. Saito, K. Tsushima, A. W. Thomas and A. G. Williams, Phys. Lett. B **433**, 243 (1998)